SWIFT-XRT-CALDB-09

Release Date: April 28th, 2006

Prepared by : Sergio Campana[1], Andrew P. Beardmore[2], Giancarlo Cusumano[3], Oliver Godet[2]

Date Revised: 28 April 2006

Revision : 1.0

Revised by: Sergio Campana

Pages Changed: all

[1]INAF-OAB , [2]Leicester University, [3]INAF-IASF Palermo

SWIFT XRT CALDB RELEASE NOTE SWIFT-XRT-CALDB-09: Response matrices and Ancillary Response Files

1. Component Files:

Filename	Mode	Grade	Date
swxwt0to2_20010101v008.rmf swxwt0to2_20010101v008.arf	WT	0-2	04/27/06
swxwt0_20010101v008.rmf swxwt0_20010101v008.arf	WT	0	04/27/06
swxpc0to12_20010101v008.rmf swxpc0to12_20010101v008.arf	PC	0-12	04/27/06
swxpc0_20010101v008.rmf swxpc0_20010101v008.arf	PC	0	04/27/06
swxpd0to5_20010101v007.rmf *swxpd0to5_20010101v003.arf*	*LRPD*	*0-5*	*04/05/2005* *07/04/2005*
swxpd0to2_20010101v007.rmf *swxpd0to2_20010101v003.arf*	*LRPD*	*0-2*	*04/05/2005* *07/04/2005*
swxpd0_20010101v007.rmf *swxpd0_20010101v003.arf*	*LRPD*	*0*	*04/05/2005* *07/04/2005*

2. Scope of Document

This note describes the release of the Swift XRT redistribution matrix (RMF v8) and ancillary response (ARF v8) files. Files are released for each working XRT mode (Photon Counting, PC, Window Timing, WT) and two different grade selections for each mode[1]. The XRT effective area is made by three main components: the mirror effective area, the CCD quantum efficiency (QE) and the filter transmission. The QE is included directly in the redistribution matrix. The ARF files contain the mirror effective area, the filter transmission, as well as the vignetting correction and the Point Spread Function (PSF) correction (which depends on the source location and of the size of the extraction region). Here we report on the CALDB RMF and ARF files which represent the effective area of the telescope for a nominal on-axis observation (no vignetting correction) and for an infinite region of interest (no correction for PSF losses). RMF files do not include the PSF correction and do not depend on the source position on the detector. The CCD soft energy response is sufficiently uniform within the central 200x200 pixels (see e.g. previous RMF release notes), therefore there is just one RMF file per mode and grade selection. The ARF files instead need vignetting and PSF corrections and therefore need to be built for each observation. To produce the observation-specific ARF files, the *xrtmkarf* task (XRTDAS-HEADAS software) has been developed. This task corrects the nominal ARF file for the vignetting and, optionally (default=yes), for PSF losses. The adopted calibration method implies that in the CALDB ARF files we include the residual correction of the CCD quantum efficiency. This explains why the nominal ARF files are different for different grade selection.

3. RMF generation

The Response Matrix Files (RMFs) are created by a Monte-Carlo simulation code (Osborne et al. 2005, SPIE 5859 340). This code models: transmission of the incident X-rays through the CCD electrode structure; photo-absorption in the active layers of the device; charge cloud generation, transportation and spreading; silicon fluorescence and its associated escape peak; surface loss effects; mapping of the resultant charge-cloud to the detector pixel array; charge transfer efficiency; addition of electronic read-out noise; event thresholding and classification according to the specific mode of operation. In orbit observations of the soft calibration sources were used to refine the surface loss function in order to better match the spectral redistribution at low energies. For heavily absorbed sources, the parametrization of the redistribution of high energy X-rays down to low energies was improved slightly for PC mode, and will be improved in the next release for WT mode (see Future Prospects, below). Also for this release, the electronic noise contribution has been increased compared with that expected from ground calibrations because of the higher than expected operating temperatures resulting from the failure of the XRT thermoelectric cooler.

---

[1] Files for the Low Rate PhotoDiode mode were not updated after the XRT CCD was damaged by a micro-meteorite, resulting in the loss of this operational mode. For this mode the older (rmf v7 and arf v3 response) can be used. We do not update PC response for grade 0-4 too. Testing has been carried out extensively on WT grade 0-2 and PC 0-12 and only in a limited way for the single pixel response.

4. ARF generation

In order to model the overall XRT response we used the latest RMF matrices (hereby released) and a new mirror effective area file (*sweffarea20010101v003.fits* which is based on a better description of the XRT mirror spider support design and also uses updated gold reflectivity tables) and fine tune the ARF files on the X-ray spectra from different celestial sources.

Crab-like supernova remnants are sources characterized by well known energy spectral distributions, stable with time. Thanks to these characteristics these objects are the best candidates for in-flight calibration of the global effective area of X-ray telescopes. Crab nebula and PSR B0540-69 have been used to calibrate the XRT effective area for the two XRT observing modes at this stage, together with other stable sources like isolated neutron stars (RX J1856-38 and RX J0720-31) and the cluster of galaxies PKS 0745-19. We also used simultaneous observations with XMM-Newton on 3C 273 and H1426+428. In addition to this process, we compare the absolute flux (as well as their spectrum) of several calibration sources with spectra taken with the XMM-Newton MOS in order to improve the absolute flux determination both in WT and PC modes (as well as the same source in WT and PC in order to gain consistency between the two). A comparison between the effective areas of the previous released matrices and the new ones can be found in Fig. 1. Previous matrices provided flatter spectra with a <0.1 difference in photon index.

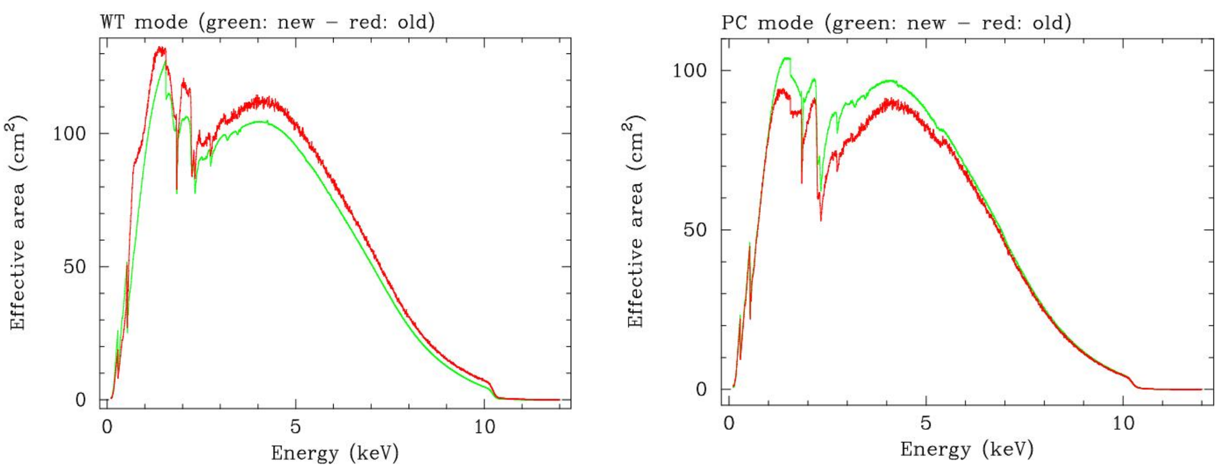

Figure1 : XRT effective area for WT grade 0-2 (left) and PC grade 0-12 (right) observing modes.

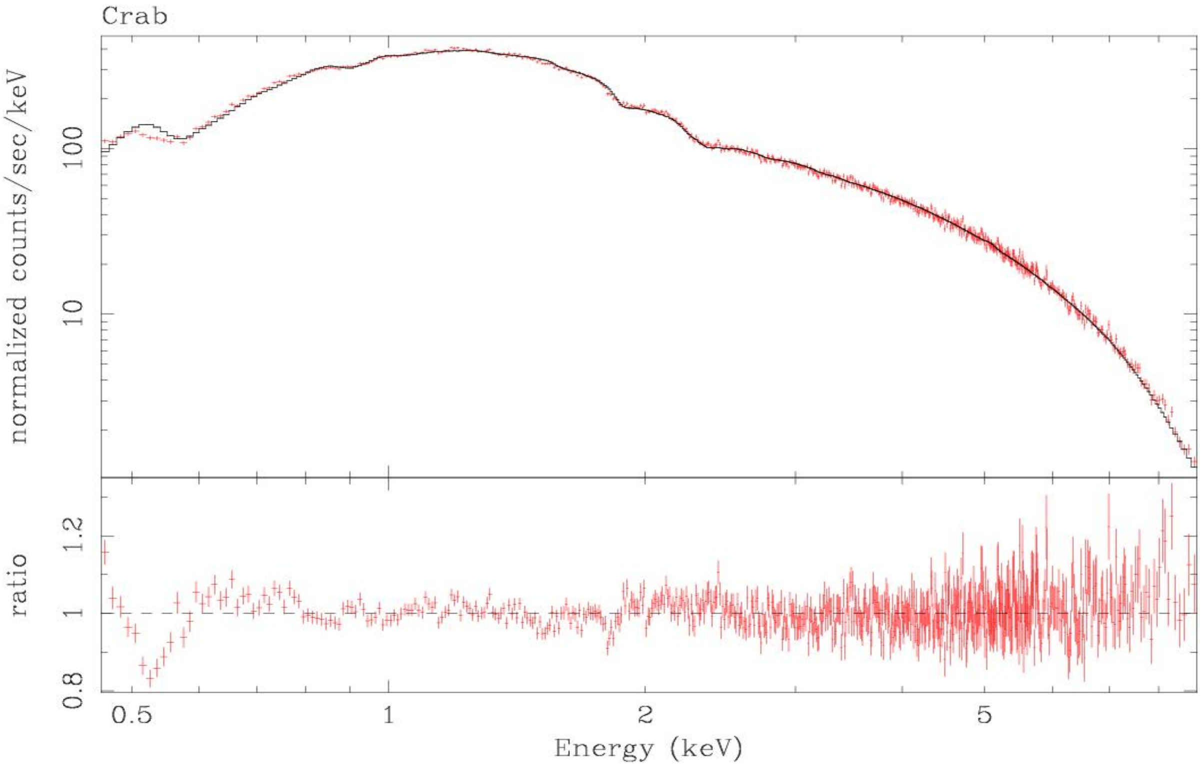

Figure 2: WT residuals of the Crab spectrum (grade 0-2). The spectrum has been rebinned to have 100 counts per energy bin.

• In the case of the WT mode we mainly used the Crab nebula as calibrator, but in this case we have to deal with a moderate pile-up in the Crab. This is almost fully mitigated using the off-pulse spectrum (which has a lower count rate). Figure 2 shows the residuals obtained by fitting the Crab nebula with an absorbed power law plus absorption features (Ne, O and Fe) outlined in Kirsch et al. (2005, SPIE 5859, 22). The fit is carried out in the 0.45-9 keV energy range and it is relatively good with a reduced chi-squared χ^2_{red} =1.83 (620 degrees of freedom, dof). This energy range was used because an increase in the residuals seen in the low energy part of the spectrum below 0.45 keV. This increase is due to redistribution matrix problems (see Section 4 below) which are enhanced by some residual pile-up at high energies. We estimate a mean systematic uncertainty at a level of 3% in the 0.3-10 keV energy range (this is the systematic uncertainty to be added in order to obtain a χ^2_{red} =1.0 spectrum). The strongest features visible in the Crab spectrum are absorption features around 0.5 keV (Oxygen), 1.5 keV (Aluminum, from the filter) and 1.8 keV (Silicon). There is also some instrumental Nickel contamination present in the 7-8 keV energy range which (sometimes) is not fully subtracted. In addition, we also show the spectrum of the AGN 3C 273 (0.3-10 keV) in order to better highlight the 0.5 keV feature connected with the Oxygen edge (see Fig. 3). This fit has been obtained by fitting together XMM-Newton and Swift data. The edge-like residuals could be due to energy scale offsets (see also Section 4 below).
In conclusion, we recommend to fit XRT WT spectra in the 0.3-10 keV energy range with these updated XRT response.

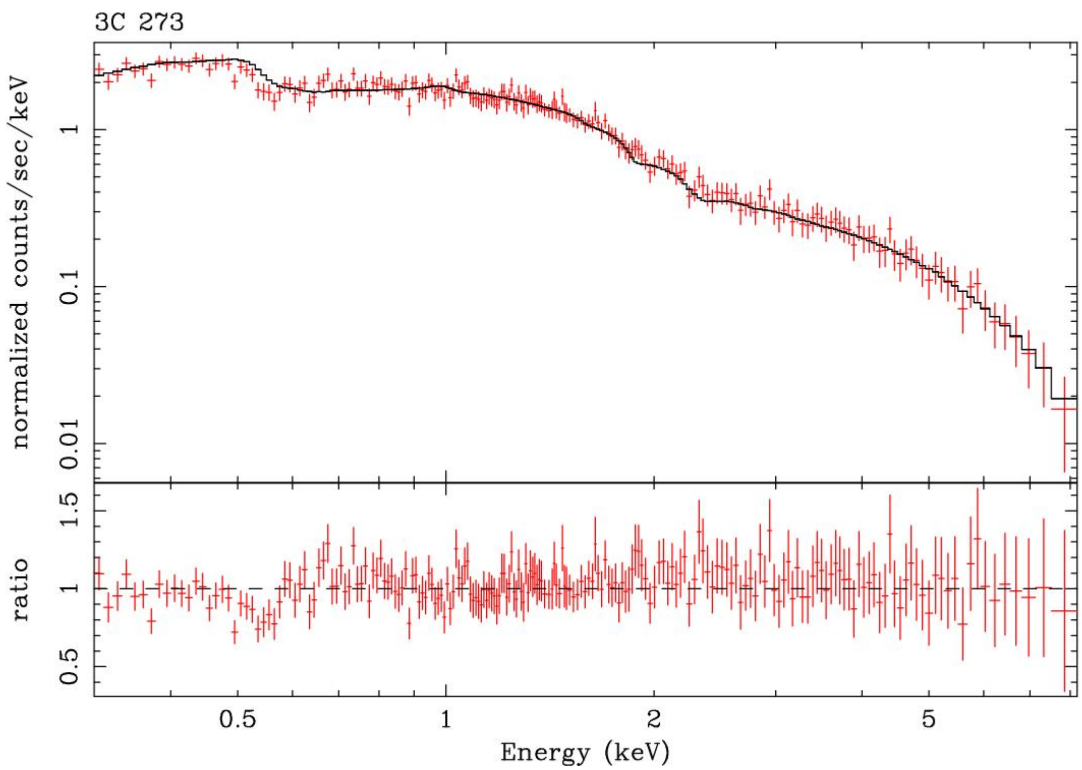

Figure 3: WT residuals of 3C273 spectrum (grade 0-2).

• In PC mode the ancillary files are calibrated with the Crab-like plerion PSR B0540-69 as well as the isolated neutron star RX J0720-31, the cluster of galaxies PKS0745-19 and the quasar H1426+428 (observed simultaneously with XMM-Newton, see Figure 4). Some of these sources are shown below. For all of these sources we obtain good fits (binning the data to 100 counts per bin) fitting together the Swift XRT spectra with XMM-Newton MOS spectra (not shown).

Source	χ^2_{red} (XRT)	χ^2 (dof)
PSR B0540-69	0.77	105.8 (138)
RXJ 0720-31	1.03	31.9 (31)
PKS0745-19	0.50	134.9 (273)
H1426+428	1.40	136.9 (98)

These fits have been obtained fitting together Swift XRT data together with XMM-Newton MOS data and then evaluating the χ^2 fixing the spectral model and fitting only the XRT data. The addition of a constant factor allows us to estimate the goodness of the absolute calibration.

The strongest features in the PSR 0540-69 spectrum are an absorption feature at ~0.5 keV (Oxygen) and an emission feature at slightly higher energies. This feature is large and might be related to the source itself as XMM-Newton spectra might indicate. Smaller features at larger energies are also present. Similar residuals are also found in our calibration sources (see Fig. 4). In addition, we shown the spectrum of the soft isolated neutron star RX J0720-31, showing that our response is now able to well reproduce its spectrum down to 0.3 keV.

The statistical uncertainty on the final RMF+ARF matrices in PC mode is estimated at 3% level in the 0.3-10 keV energy range.

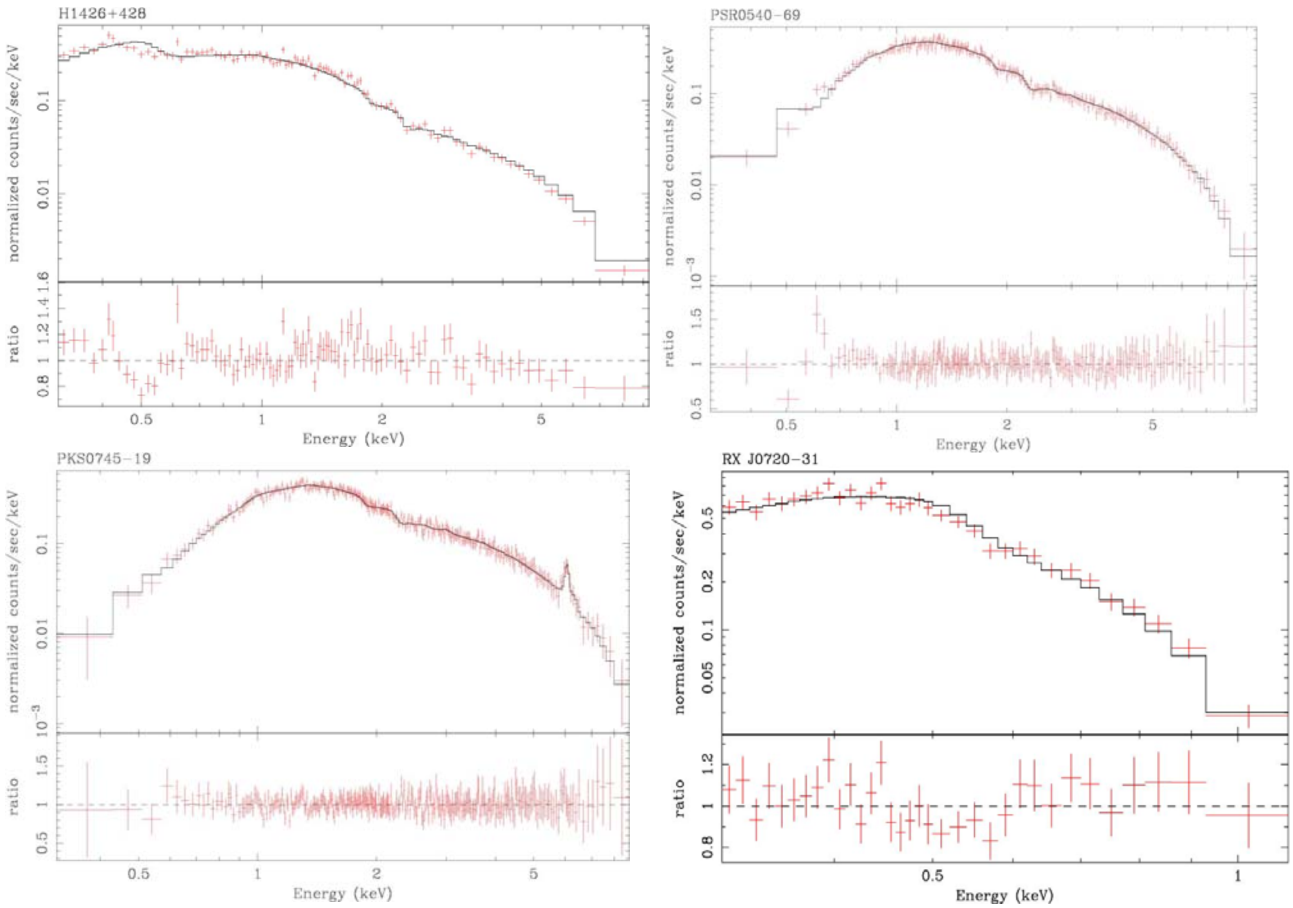

Figure 4: XRT spectrum (grade 0-12) of H1426+426, PSR B0540-69, PKS0745-19 and RX J0720-31 in PC mode (upper panel) together with its residuals (lower panel).

5. Current limitations and future prospects

Our current understanding of the XRT response still implies a systematic uncertainty of the order of 3% in the 0.3-10 keV energy band (recommended band to be used) and of about 10% in absolute flux. The following considerations apply to both WT and PC mode observations.

- For highly absorbed sources the response model showed an under-estimation of the redistribution below about 1 keV. The parametrization of this loss-shelf has been improved but needs further refinements. The problem is clearly evident for N_H>10^{22} cm^{-2} but even for less absorbed sources small deviations are present. This however did not affect significantly the spectral parameters.
- We are starting observing a degradation of the charge transfer inefficiency (CTI), from 80 eV FWHM to 105 eV FWHM at 1.8 keV (based on Cas A spectra) and new response matrices will have to account for this worsening of the spectral resolution.
- Especially in case of bright sources we do experience small energy scale (ΔE) problems at low energies (E <1 keV, i.e. when ΔE/E < 0.1 keV, see Fig. 5). This

problem is still under investigation and might be related to bright Earth contamination in PC mode and a bias subtraction problem in WT mode, causing energy scale offsets. Fitting these spectra with the "gain fit" command within XSPEC (only an offset) increases the quality of the fits, but these offsets can be as large as -80 eV. This can be mitigated with the option *wtbiasdiff* in *xrtpipeline* (in the case of WT mode).

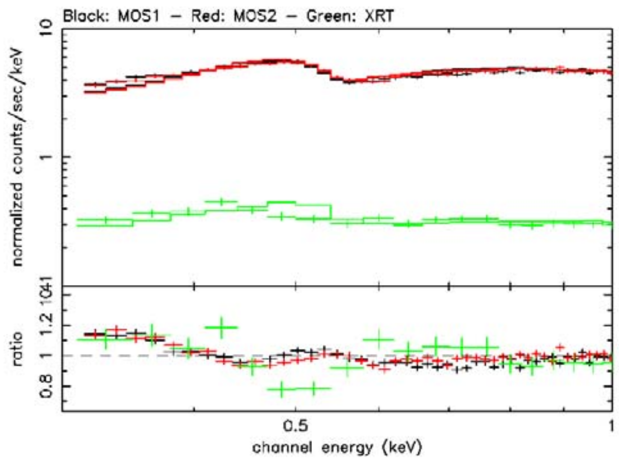

Figure 5: Simultaneous fit of XMM-Newton (red) and Swift XRT (green) spectra of H1426+428, highlighting the energy scale problem in the 0.5 keV energy region.

- A multi-mission, simultaneous observational campaign was performed on 3C 273. Fig. 6 shows the results of fitting the Swift XRT/WT, XMM MOS2 and pn, and RXTE PCA spectra with a power-law and black body components for the soft excess. The XRT photon index and flux compare well to the other instruments, with an absolute flux calibration better than 10%. This flux calibration, with respect to XMM-Newton MOS, has been confirmed using several sources.

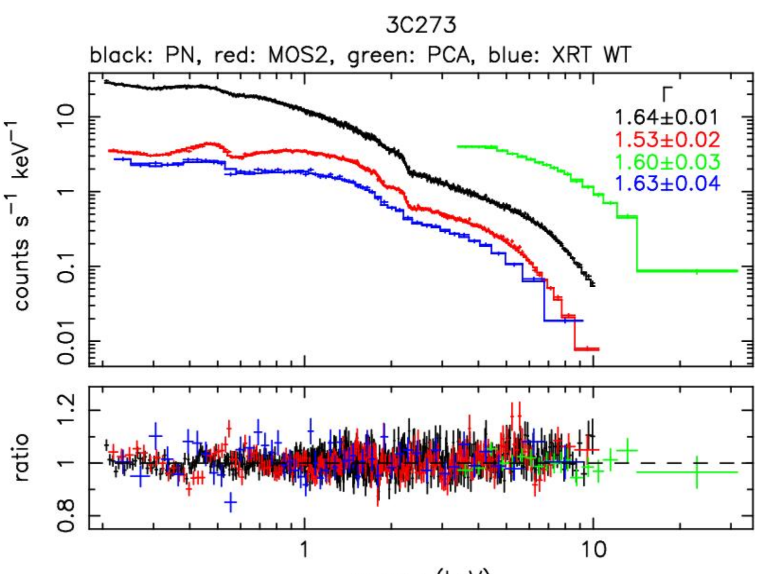

Figure 6: XRT spectrum (grade 0-12) of 3C273 (blue) together with XMM-PN (black), XMM-MOS2 (red) and RXTE-PCA (green) spectra. Normalizations were allowed to vary and are all within 10%.